

Seasonal variability in the light absorption properties of western Arctic waters: Parameterization of the individual components of absorption for ocean color applications

Atsushi Matsuoka,¹ Victoria Hill,² Yannick Huot,³ Marcel Babin,^{1,4} and Annick Bricaud¹

Received 23 June 2009; revised 12 November 2010; accepted 7 December 2010; published 8 February 2011.

[1] The light absorption properties of particulate and dissolved materials strongly influence the propagation of visible light in oceanic waters and therefore the accuracy of ocean color algorithms. While the general absorption properties of these materials have been reported for Arctic waters, their seasonal variability remains unknown. We investigated the light absorption coefficients of phytoplankton [$a_{\phi}(\lambda)$], nonalgal particles [$a_{\text{NAP}}(\lambda)$], and colored dissolved organic matter [$a_{\text{CDOM}}(\lambda)$] in both coastal and oceanic waters of the western Arctic Ocean from spring to autumn. Values for the chlorophyll *a*-specific absorption coefficient of phytoplankton [$a_{\phi}^*(440)$] declined significantly from the ice melt period in the early spring to the summer. Using high-performance liquid chromatography, we show that the decrease in $a_{\phi}^*(440)$ was due to a strong package effect that overwhelmed the influence of the pigment composition. A decrease in the $a_{\text{NAP}}(\lambda)$ values from spring and summer to autumn likely originated from a decrease in the concentration of phytoplanktonic detritus. The $a_{\text{CDOM}}(\lambda)$ near the surface decreased by 34% from spring to summer as a result of photobleaching by solar radiation. The colored dissolved organic matter (CDOM) absorption values then increased significantly during autumn, resulting from the cumulative injection of Alaskan Coastal Waters into the Arctic as well as CDOM generated in situ. Our results suggest that all of the absorption components are tightly linked to biogeochemical processes, and thus the seasonal variability in $a_{\phi}(\lambda)$, $a_{\text{NAP}}(\lambda)$, and $a_{\text{CDOM}}(\lambda)$ should be taken into account in bio-optical models.

Citation: Matsuoka, A., V. Hill, Y. Huot, M. Babin, and A. Bricaud (2011), Seasonal variability in the light absorption properties of western Arctic waters: Parameterization of the individual components of absorption for ocean color applications, *J. Geophys. Res.*, 116, C02007, doi:10.1029/2009JC005594.

1. Introduction

[2] The western Arctic Ocean has recorded the most significant reduction in summer sea ice cover and the greatest increase in sea surface temperature warming anomalies of any Arctic region since the late 1970s [e.g., Shimada *et al.*, 2006; Perovich *et al.*, 2007; Stroeve *et al.*, 2008]. Because this area is highly productive [Chen *et al.*, 2002; Hill and Cota, 2005], concern over the impact of these changes on the physical environment (e.g., solar irradiation, strengthening stratification, etc.), possibly leading to modifications in biogeochemical processes, is at the forefront of Arctic

research. However, the remoteness of the Arctic Ocean impedes our understanding of this extreme environment because in situ data remain sparse in time and space [Sakshaug, 2004]. Remote sensing provides an attractive alternative to in situ observations by enabling the investigation of the temporal and spatial patterns of biogeochemical processes occurring in this dynamic environment.

[3] Since light absorption properties are tightly linked to biogeochemical processes [e.g., Morel, 1988, 1991], the measurement of ocean color using space-based radiometers such as the Sea-viewing Wide Field-of-view Sensor (SeaWiFS), the Moderate Resolution Imaging Spectroradiometer (MODIS), and the Medium-Resolution Imaging Spectrometer (MERIS) allows us to examine changes in the Arctic ecosystem. Beyond tracking phytoplankton biomass, perhaps the most important contribution that these sensors can potentially offer is estimations of water column primary production (PP), which is essential for understanding changes occurring in the Arctic ecosystem. This long-term goal underscores the importance of advancing our knowledge of the optical characteristics of Arctic waters.

[4] Algorithms exist which use spectral variations in remotely sensed ocean color reflectance to estimate PP [e.g.,

¹Laboratoire d'Océanographie de Villefranche, Université Pierre et Marie Curie, Centre National de la Recherche Scientifique, Villefranche-sur-Mer, France.

²Ocean, Earth, and Atmospheric Sciences, Old Dominion University, Norfolk, Virginia, USA.

³Centre d'Applications et de Recherches en Télédétection, Département de Géomatique Appliquée, Université de Sherbrooke, Sherbrooke, Quebec, Canada.

⁴Now at Québec-Océan, Université Laval, Québec City, Québec, Canada.

Platt and Sathyendranath, 1988; Sathyendranath et al., 1991; Longhurst et al., 1995; Antoine and Morel, 1996; Behrenfeld and Falkowski, 1997; Arrigo et al., 1998; Behrenfeld et al., 2005; Pabi et al., 2008]. Such PP algorithms require (1) measures of the biomass of phytoplankton, generally in the form of chlorophyll *a* (chl *a*) concentration; (2) the irradiance present in the water column; and (3) estimates of the efficiency with which phytoplankton utilize this irradiance. Obtaining accurate estimates of the efficiency of light utilization by phytoplankton remains the greatest hurdle before achieving accurate global estimates of primary production and this aspect will not be examined here. While in most oceanic waters estimates of phytoplankton biomass and of the light field are now fairly well constrained, the limited knowledge about the optical properties of Arctic waters and their variability in time remains problematic for PP estimates.

[5] Arctic waters are significantly different from temperate waters. On average, the relative contribution of phytoplankton absorption to the total nonwater absorption in the Arctic is only 16% at 440 nm where phytoplankton absorption is maximal [Matsuoka et al., 2007]. In contrast, the contribution of absorption by colored dissolved organic matter (CDOM) is remarkably high in the Arctic, and over 76% of the total nonwater absorption at 440 nm is accounted for by this absorption component [Matsuoka et al., 2007, 2009]. The strong contribution of CDOM absorption is consistent with the fact that the Arctic Ocean receives the largest amount of freshwater relative to its volume (11% of global freshwater input while its volume is only 1% of the global ocean [Shiklomanov, 1993]). It is likely that CDOM absorption plays an important role in the distribution of heat storage with depth particularly in the western Arctic Ocean [Hill, 2008], thereby potentially impacting sea ice cover in these regions. The western Arctic Ocean also receives large amounts of water containing suspended matters or nonalgal particles (NAP) delivered not only from the Mackenzie River but also from the Bering Sea [Holmes et al., 2002; Carmack et al., 2004]. Inflows of these waters show large seasonal variability [Holmes et al., 2002], and this may strongly impact local biogeochemical processes.

[6] Because of the different concentrations and natures of the constituents of Arctic waters, as well as the presence of strong coastal to open ocean gradients, it was shown that empirical algorithms for estimating the chl *a* concentration do not perform well in this environment even if they were developed expressly for Arctic waters [Matsuoka et al., 2007]. In particular, it was found that owing to the highly heterogeneous optical characteristics of Arctic waters [Retamal et al., 2008] algorithms developed specifically for the Arctic such as Arctic OC4L [Cota et al., 2004], while significantly better than a standard global algorithm (i.e., OC4V4), perform poorly when coastal waters are included [Matsuoka et al., 2007]. To address this issue, one possible approach is to use semi-analytical models, which are inherently more flexible for retrieving phytoplankton biomass compared to purely empirical algorithms. After some modification for its application to Arctic waters, the use of one such model called the quasi-analytical algorithm (QAA) [Lee et al., 2002] to retrieve $a_{\phi}(\lambda)$ values (and chl *a* concentration) seems to be a promising approach [Matsuoka, 2008]. This model relies on the observation that, for a given season, when integrated over the euphotic zone the same relationship between the chl *a*

concentration and $a_{\phi}(\lambda)$ at 440 nm can be applied to both coastal and oceanic water environments in the entire western Arctic Ocean [Matsuoka et al., 2009]. However, since phytoplankton absorption shows large changes seasonally [e.g., Stramska et al., 2006], the seasonal variability of Arctic waters needs to be examined first. This work is also useful for developing ocean color algorithms for the Arctic Ocean.

[7] For estimating PP in the Arctic Ocean, the appropriate calculation of photosynthetically usable radiation (PUR [Morel, 1978]) is critical. PUR is the light utilized by phytoplankton in photosynthetic processes [Morel, 1991], and it depends on both the spectra of phytoplankton absorption and the available irradiance. The absorption properties of Arctic waters have not yet been sufficiently documented (see discussion by Matsuoka et al. [2009]). Recent studies show that the phytoplankton absorption coefficients for Arctic waters tend to be lower compared to those at lower latitudes [Wang et al., 2005; Matsuoka et al., 2007]. As for Southern Ocean waters, this difference has been thought to be mainly due to the presence of large-sized phytoplankton featuring more limited trough-to-peaks changes in their absorption spectra and lower chlorophyll specific absorption due to the package effect [Mitchell, 1992; Wang et al., 2005; Matsuoka et al., 2007]. However, there is no direct evidence that the package effect really prevails in these waters. Since a variety of phytoplankton species are present at high northern latitudes across seasons [Cota et al., 2003; Stramska et al., 2006; Lovejoy et al., 2007; Matsuoka et al., 2009], it is also expected that they show variability in their spectral absorption characteristics resulting from varying amounts of accessory pigments. However, knowledge about the sources of variability in phytoplankton absorption is still lacking. A complete description of the distribution of PUR with depth requires the diffuse attenuation coefficient of light ($K_d(\lambda)$, m^{-1}). The $K_d(\lambda)$ can be expressed as a function of the total absorption coefficient (i.e., sum of water, phytoplankton, CDOM, and NAP absorption coefficients) and scattering coefficients [e.g., Morel, 1988, 1991]. A complete description of the individual absorption coefficients is therefore necessary to understand the variability observed in $K_d(\lambda)$.

[8] The objective of the present study is to examine seasonal variability in the light absorption properties of particulate and dissolved constituents (i.e., phytoplankton, NAP, and CDOM) from the early spring ice melt to the ice-free autumn phase in western Arctic waters. To achieve this objective, we first examine phytoplankton absorption, parameterize a simple model to describe it spectrally, and make a comparison with measurements made at lower latitudes. Afterward, we carry out similar analyses for the absorption properties of CDOM and NAP.

2. Materials and Methods

[9] Sampling was conducted in the western Arctic Ocean in the area from approximately latitudes 65° to 77°N and longitudes 145° to 180°W (Figure 1). Data were collected during three cruises during the spring to autumn (from May to October): the Western Arctic Shelf Basin Interaction (SBI) spring and summer cruises in 2002 aboard the USCGS *Healy* (referred to as SBI spr: 5 May to 15 June 2002, and SBI sum: 16 July to 26 August 2002), and the autumn cruise in 2004 of the Studies on Arctic Ocean circulation linked to

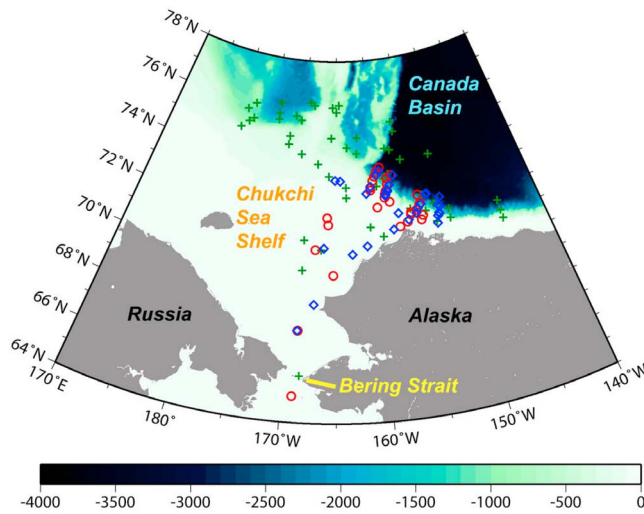


Figure 1. Location of sampling stations for the SBI spr (red circles), SBI sum (blue diamonds), and MR aut (green crosses) cruises in the western Arctic Ocean. Bathymetry is given in m.

Arctic climate system carried out by the Japanese R/V *Mirai* (referred to as MR aut: 1 September to 13 October 2004). For all cruises, temperature and light transmission profiles were obtained using a SeaBird 911 conductivity-temperature-depth (CTD) probe coupled with a transmissometer (WET Labs, Inc.).

[10] Discrete water samples were collected using Niskin bottles, except at the surface where a polyethylene container was used during the MR aut cruise. In total, 110, 119, and 179 water samples were collected at 30 (SBI spr), 29 (SBI sum), and 51 (MR aut) stations for pigment and absorption analyses within the euphotic zone (z_{eu} , m: 1% of the surface light level).

2.1. Phytoplankton Pigments

[11] In this study, chl *a* concentration was determined using three methods depending on the cruise. The chl *a* concentration was determined fluorometrically (hereafter denoted as [chl a^{flu}]) with 90% acetone [Holm-Hansen *et al.*, 1965] for SBI spr and SBI sum and with dimethylformamide (DMF) [Holm-Hansen *et al.*, 1965; Suzuki and Ishimaru, 1990] for MR aut using a 10-AU field fluorometer (Turner Designs). The duration of the extraction was approximately 24 h for 90% acetone and a minimum of three hours for DMF. With the DMF extraction, the chl *a* concentration was shown to be identical to that using 90% acetone [Suzuki and Ishimaru, 1990]. For SBI spr and SBI sum, the chl *a* concentration was also determined using high-performance liquid chromatography (HPLC) (hereafter denoted as [chl a^{HPLC}]) which includes the concentrations of chl *a*, divinyl-chl *a*, chlorophyllid *a*, and phaeopigments).

[12] We followed the standard protocols for HPLC analysis of phytoplankton samples [Wright *et al.*, 1991; Bidigare and Trees, 2000]. Samples were filtered through Whatman GF/F glass fiber filters and stored in a freezer at -40 to -80°C until analysis. Phytoplankton pigments were extracted in 100% acetone and sonicated to disrupt the cells. Pigments

were separated on an ODS-2 C18 column using a ThermoQuest UV6000 scanning diode array detector (190 to 800 nm with 1 nm intervals) as the absorption detector. In addition, a ThermoQuest FL3000 scanning fluorescence detector was used to detect and quantify the various chlorophyll degradation products, which occur at lower concentrations.

[13] To examine the variability in pigment compositions, we grouped the accessory pigments into four categories: (1) chlorophyll *b* (denoted as chl *b*); (2) chlorophyll c_1 , c_2 , and c_3 (denoted as chl *c*); (3) photosynthetic carotenoids (denoted as PSC) consisting of fucoxanthin, peridinin, 19'-HF, and 19'-BF; and (4) nonphotosynthetic carotenoids (denoted as NPC) consisting of zeaxanthin, diadinoxanthin, alloxanthin, and β -carotene.

2.2. Absorption

[14] We followed the NASA ocean color protocols for particulate and dissolved absorption measurements [Mitchell *et al.*, 2003]. Water samples were filtered under low vacuum on Whatman GF/F glass fiber filters immediately after water sampling. Optical density (OD, dimensionless) of all particles on these filters, referred to as $\text{OD}_p(\lambda)$ (subscript *p* denotes phytoplankton plus NAP), was then measured from 350 to 750 nm with 2 nm intervals for both SBI spr and SBI sum, and with 1 nm intervals for MR aut, using an MPS-2400 spectrophotometer (Shimadzu corp.). Phytoplankton pigments were extracted using methanol [Kishino *et al.*, 1985] and the OD of NAP, referred to as $\text{OD}_{\text{NAP}}(\lambda)$, was measured in the same way as for $\text{OD}_p(\lambda)$. The baseline correction was accomplished by subtracting the OD of a fully hydrated blank filter from $\text{OD}_p(\lambda)$ and $\text{OD}_{\text{NAP}}(\lambda)$. Using the coefficients for the β correction as proposed by Cleveland and Weidemann [1993], we converted these OD values into absorption coefficients for total particles ($a_p(\lambda)$, m^{-1}) and NAP ($a_{\text{NAP}}(\lambda)$, m^{-1}) using the averages of the measured values between 746 and 750 nm ($\text{OD}_{\text{null},j}$, dimensionless) for the null correction:

$$a_j(\lambda) = 2.303 \frac{A \times [\text{OD}_j(\lambda) - \text{OD}_{\text{null},j}]}{\beta \times V}, \quad (1)$$

where *j* denotes either total particles (*p*) or NAP retained on the filter. The coefficient 2.303 is a factor for converting base *e* to base 10 logarithms, *A* is the clearance area of the filter (in m^2), and *V* is the sample volume (in m^3). We finally obtained absorption coefficients of phytoplankton ($a_\phi(\lambda)$, m^{-1}) by subtracting $a_{\text{NAP}}(\lambda)$ from $a_p(\lambda)$:

$$a_\phi(\lambda) = a_p(\lambda) - a_{\text{NAP}}(\lambda). \quad (2)$$

[15] Regression analysis was conducted to determine the relationship between $a_\phi(\lambda)$ and [chl a^{flu}] from 400 to 700 nm with 5 nm intervals, as in the work of Bricaud *et al.* [1998]:

$$a_\phi(\lambda) = A_\phi(\lambda) [\text{chl } a]^{\text{B}_\phi(\lambda)}, \quad (3)$$

where $A_\phi(\lambda)$ and $\text{B}_\phi(\lambda)$ are the regression coefficients derived from our data set. The chl *a*-specific absorption coefficient of phytoplankton, $a_\phi^*(\lambda)$ ($\text{m}^2 \text{mg}^{-1}$), was calculated by dividing $a_\phi(\lambda)$ by [chl *a*].

[16] For the absorption measurements of CDOM, water samples were filtered using 0.22 μm Millipore membranes immediately after water sampling and then poured into a 0.1 m quartz cell. The OD of CDOM, $OD_{\text{CDOM}}(\lambda)$, was obtained from a scan from 280 to 700 nm with 2 nm intervals for SBI spr and SBI sum and with 1 nm intervals for MR aut, using a MPS2400 spectrophotometer (Shimadzu corp.). A baseline correction was applied by subtracting the OD of MilliQ water from $OD_{\text{CDOM}}(\lambda)$. The average of the measured values of $OD_{\text{CDOM}}(\lambda)$ over 5 nm interval around 685 nm ($OD_{\text{null,CDOM}}$, dimensionless) was assumed to be 0 and the $OD_{\text{CDOM}}(\lambda)$ spectrum was shifted accordingly [Babin *et al.*, 2003]. We finally obtained $a_{\text{CDOM}}(\lambda)$ (m^{-1}) as follows:

$$a_{\text{CDOM}}(\lambda) = 2.303 \frac{[OD_{\text{CDOM}}(\lambda) - OD_{\text{null,CDOM}}]}{0.1}, \quad (4)$$

where 2.303 is a factor for converting base e to base 10 logarithms and 0.1 is the optical path length (in m). The total nonwater absorption coefficient, $a_{\text{t-w}}(\lambda)$ (m^{-1}), was then calculated as the sum of $a_{\varphi}(\lambda)$, $a_{\text{NAP}}(\lambda)$ and $a_{\text{CDOM}}(\lambda)$.

[17] Spectra of $a_{\text{NAP}}(\lambda)$ and $a_{\text{CDOM}}(\lambda)$ can be expressed as exponential functions as follows [e.g., Bricaud *et al.*, 1981; Babin *et al.*, 2003]:

$$a_i(\lambda) = a_i(\lambda_r) e^{(-S_i(\lambda - \lambda_r))}, \quad (5)$$

where i expresses either NAP, CDOM, or CDM (=NAP + CDOM), λ_r is the reference wavelength (i.e., 440 nm in this study), and S_{NAP} , S_{CDOM} , and S_{CDM} denote the spectral slopes for NAP, CDOM, and CDM absorption, respectively. S_{NAP} was calculated by fitting a nonlinear model to the data from 380 to 730 nm, excluding the 400–480 and 620–710 nm ranges to avoid any residual pigment absorption that might still have been present [Babin *et al.*, 2003]. S_{CDOM} was calculated by fitting a nonlinear model to the data from 350 to 500 nm [Babin *et al.*, 2003] (see also Appendix A). S_{CDM} was calculated by fitting a nonlinear model to the data from 380 to 500 nm, excluding the 400–480 nm range.

2.3. Calculation for the Package Effect and Pigment Composition of Phytoplankton

[18] We calculated $Q_a^*(\lambda)$ (dimensionless) as a proxy of the package effect, following Bricaud *et al.*'s [1995, 2004] method:

$$Q_a^*(\lambda) = \frac{a_{\varphi}(\lambda)}{a_{\text{pigment}}(\lambda)}, \quad (6)$$

$$a_{\text{pigment}}(\lambda) = \sum C_i a_{\text{sol},i}^*(\lambda), \quad (7)$$

where $a_{\text{sol},i}^*(\lambda)$ denotes weight-specific absorption spectra of individual pigments (in $\text{m}^2 \text{mg}^{-1}$) presented by Bricaud *et al.* [2004]. The C_i values are the concentrations of the individual pigments in solution (in mg m^{-3}) and were measured using HPLC (see section 2.1).

[19] It is generally observed that $a_{\text{pigment}}(\lambda)$ computed by equation (7) underestimates the total pigment absorption in solution at some wave bands [see Bricaud *et al.*, 2004]. If

we define this missing absorption as $a_{\text{miss}}(440)$ (m^{-1}), then equation (6) can be rewritten as follows:

$$cQ_a^*(440) = \frac{a_{\varphi}(440)}{[a_{\text{pigment}}(440) + a_{\text{miss}}(440)]}, \quad (8)$$

where

$$a_{\text{miss}}(440) = 0.0525[\text{chl } a]^{0.855}. \quad (9)$$

Coefficients for $a_{\text{miss}}(440)$ values were given by Bricaud *et al.* [2004]. The term $cQ_a^*(440)$ denotes a corrected- $Q_a^*(440)$. To examine a potential bias for $a_{\text{miss}}(440)$ as a function of the chl a concentration, we also calculated $Q_a^*(\lambda)$ at 676 nm where chl a strongly dominates compared to other accessory pigments, simply following equations (6) and (7) (see section 3.1.1 for details). In order to examine the effect of the pigment composition, the chl a -specific $a_{\text{pigment}}(440)$ (referred to as $a_{\text{pigment}}^*(440)$ ($\text{m}^2 \text{mg}^{-1}$)) was obtained by dividing $a_{\text{pigment}}(440)$ by $[\text{chl } a^{\text{HPLC}}]$.

2.4. Statistical Analyses

[20] In the present study, we examined a difference in mean values for each pair of optical parameters with the statistical significance according to the criteria as follows [Sokal and Rohlf, 1973]. If the normality of the distributions was verified for a variable using a Kolmogorov-Smirnov test, we then conducted either a T-test (two variables) or an ANOVA (three variables). Prior to statistical testing, the data were log-transformed according to Campbell [1995] for the chl a concentration, $a_i(440)$ (where i expresses either phytoplankton (φ), CDOM, or NAP), and $a_{\varphi}^*(440)$; log transformation was not performed for $cQ_a^*(440)$, $Q_a^*(676)$, and $a_{\text{pigment}}^*(440)$. In addition, if a significant difference was identified by the ANOVA test, the data were subjected to a TukeyHSD multiple comparison in order to examine which pairs of parameters were statistically different. If a variable was not normally distributed, as was the case for $cQ_a^*(440)$, $Q_a^*(676)$, and $a_{\text{pigment}}^*(440)$, we conducted a nonparametric Wilcoxon rank sum test (see section 3.1.1). We also conducted an F test to examine the difference in variances for each pair of optical relationships.

3. Results and Discussion

[21] The chl a concentration varied widely across seasons. Mean values of $[\text{chl } a^{\text{fluor}}]$ increased significantly from spring to summer ($p < 0.0001$, ANOVA plus TukeyHSD test; Figure 2). Higher chl a concentrations in summer (geometric mean: 0.553 mg m^{-3} , geometric SD: 3.000) than in spring (geometric mean: 0.300 mg m^{-3} , geometric SD: 2.375) resulted from the fact that we did not experience the true spring bloom that occurred sometime between the end of the SBI spring cruise and the beginning of the SBI summer cruise (see discussion by Hill *et al.* [2005]). Mean values of $[\text{chl } a^{\text{fluor}}]$ then decreased significantly from summer to autumn (geometric mean: 0.373 mg m^{-3} , geometric SD: 2.787) ($p < 0.001$, ANOVA plus TukeyHSD test; Figure 2). This seasonal variability influences that of $a_{\varphi}^*(440)$ (see section 3.1.1 for details).

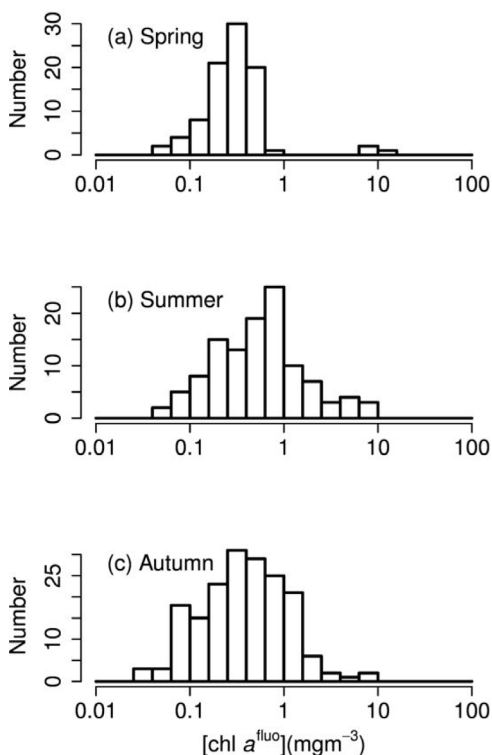


Figure 2. Histograms of $[\text{chl } a^{\text{fluo}}]$ for (a) spring, (b) summer, and (c) autumn.

3.1. Phytoplankton Absorption

3.1.1. Seasonal Variability

[22] A significant coefficient of determination between $a_{\phi}(\lambda)$ at 440 nm and $[\text{chl } a^{\text{fluo}}]$ was found for all samples across the seasons (spring, summer and autumn) ($r^2 = 0.71$, $p < 0.0001$, $N = 384$; Figure 3). The regression for all data points (black solid curve) showed a similar trend compared to those obtained at lower latitudes [Bricaud et al., 1998] and in the Labrador Sea [Cota et al., 2003] at various seasons. A systematic difference exists between the $a_{\phi}(440)$ versus $[\text{chl } a^{\text{fluo}}]$ relationship observed here and that reported by Wang et al. [2005] for the same study region. However, we cannot determine the origin of this difference because a detailed study of the phytoplankton community was not conducted together with the summer observations of Wang et al. [2005].

[23] A lower coefficient of determination between $a_{\phi}(440)$ and $[\text{chl } a^{\text{fluo}}]$ was found for the spring ($r^2 = 0.63$, $N = 89$; $p < 0.0001$) compared to that for the summer and autumn ($r^2 = 0.78$ and 0.80 for $N = 114$ and 179 , respectively; $p < 0.0001$ for both). During the ice melt of the spring season, Hill et al. [2005] indicated that the phytoplankton populations were characterized by a variable mixture of phytoplankton $> 5\mu\text{m}$ (i.e., diatoms, haptophytes, and dinoflagellates) and phytoplankton $< 5\mu\text{m}$ (i.e., prasinophytes) that adapt better to cold waters under low solar irradiation. The magnitude of phytoplankton absorption differs among phytoplankton species [e.g., Bricaud and Morel, 1983; Johnsen et al., 1994]. The lower coefficient of determination found during the spring period may thus result from a more spatially heterogeneous phytoplankton species composition than in summer

and autumn, which is supported by Hill et al. [2005]. The logarithmic slope for $a_{\phi}(440)$ versus $[\text{chl } a^{\text{fluo}}]$ was significantly higher in autumn compared to spring and summer ($p < 0.0001$ for both, F test), which results from a lower absorption efficiency at low chl a concentrations ($< 1.0 \text{ mg m}^{-3}$).

[24] While no difference of the logarithmic slope for $a_{\phi}(440)$ versus $[\text{chl } a^{\text{fluo}}]$ between spring and summer was identified, there was a significant difference in the mean $a_{\phi}^*(440)$ (Figure 4). The mean value of $a_{\phi}^*(440)$ decreased significantly from spring to summer ($p < 0.0001$, ANOVA plus TukeyHSD test), and no significant difference was identified between summer and autumn. While a detailed study of the phytoplankton pigments was not conducted for the autumn cruise, there are two possible causes for the significant difference between spring and summer based upon the HPLC analysis: (1) a change in the package effect and/or (2) changes in the pigment composition [e.g., Morel and Bricaud, 1981; Bricaud et al., 1995, 2004].

[25] To examine these effects, $Q_a^*(\lambda)$, which is a proxy of the package effect, is plotted against $[\text{chl } a^{\text{HPLC}}]$ (Figure 5a). The trend of ${}_cQ_a^*(440)$ against $[\text{chl } a^{\text{HPLC}}]$ was similar to that of $Q_a^*(\lambda)$ at 676 nm where chl a dominates compared to other accessory pigments [e.g., Bidigare et al., 1990; Bricaud et al., 2004]. There was no significant difference of variances between ${}_cQ_a^*(440)$ and $Q_a^*(676)$ for spring and summer ($p = 0.45$ and 0.56 , respectively, F test). While various pigments exist at 440 nm, this result gives us confidence that ${}_cQ_a^*(440)$ calculated in this study is appropriate for evaluating the package effect.

[26] Both ${}_cQ_a^*(440)$ and $Q_a^*(676)$ values tended to decrease with increasing chl a concentrations for spring and summer (Figure 5), which is consistent with previous findings at moderate latitudes [Bricaud et al., 1995, 2004; Babin et al.,

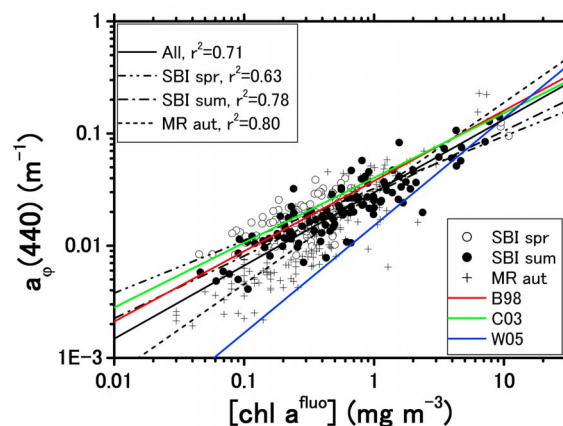


Figure 3. Relationship between $a_{\phi}(440)$ and $[\text{chl } a^{\text{fluo}}]$. Regression curves for each cruise (or season) as well as the three together are shown. For SBI spr (open circles): $a_{\phi}(440) = 0.0323[\text{chl } a^{\text{fluo}}]^{0.466}$; $r^2 = 0.63$, $p < 0.0001$, $N = 89$. For SBI sum (solid circles): $a_{\phi}(440) = 0.0293[\text{chl } a^{\text{fluo}}]^{0.557}$; $r^2 = 0.78$, $p < 0.0001$, $N = 114$. For MR aut (crosses): $a_{\phi}(440) = 0.0293[\text{chl } a^{\text{fluo}}]^{0.809}$; $r^2 = 0.80$, $p < 0.0001$, $N = 179$. Regression curves from the literature are also shown for comparison (i.e., Bricaud et al. [1998] in red, Cota et al. [2003] in green, and Wang et al. [2005] in blue).

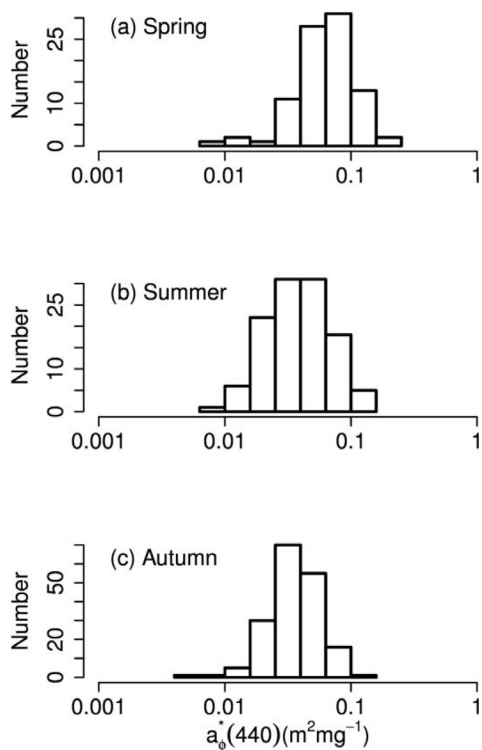


Figure 4. Histograms of $a_{\phi}^*(440)$ for (a) spring, (b) summer, and (c) autumn.

1996]. Most of those values were lower than 1 (theoretical limit), except for some samples likely affected by experimental errors (see discussion by *Bricaud et al.* [1995, 2004]). This result suggests that a strong package effect was observed in our data. While no significant difference for the semilogarithmic slopes for $cQ_a^*(440)$ or $Q_a^*(676)$ versus $[\text{chl } a^{\text{HPLC}}]$ was identified between spring and summer, values of $cQ_a^*(440)$ and $Q_a^*(676)$ in summer were on average significantly lower than in spring over the whole chl a concentration range of 0.03 to 10 mg m^{-3} ($p < 0.05$ for both; Wilcoxon rank sum test).

[27] For $a_{\text{pig}}^*(440)$, which is used as a proxy of pigment composition [*Bricaud et al.*, 2004], significantly higher values were found in summer compared to spring ($p < 0.05$, Wilcoxon rank sum test; Figure 6). This result indicates that changes in pigment composition also occurred. Here, we note that $a_{\text{pig}}^*(440)$ values increased from spring to summer, whereas both $cQ_a^*(440)$ and $Q_a^*(676)$ values decreased (Figures 5 and 6). Given the decreasing trend observed in $a_{\phi}^*(440)$ from spring to summer, those results suggest that the package effect has an overwhelming influence compared to the pigment composition in lowering $a_{\phi}^*(440)$. It is noted here that our results would not change even when values of $cQ_a^*(440)$, $Q_a^*(676)$, and $a_{\text{pig}}^*(440)$ at high chl a concentrations ($\sim 10 \text{ mg m}^{-3}$) in spring (three samples shown; see Figures 5 and 6) were excluded from our analyses.

[28] It is interesting to examine the seasonal variability in pigment composition and consider possible phytoplankton

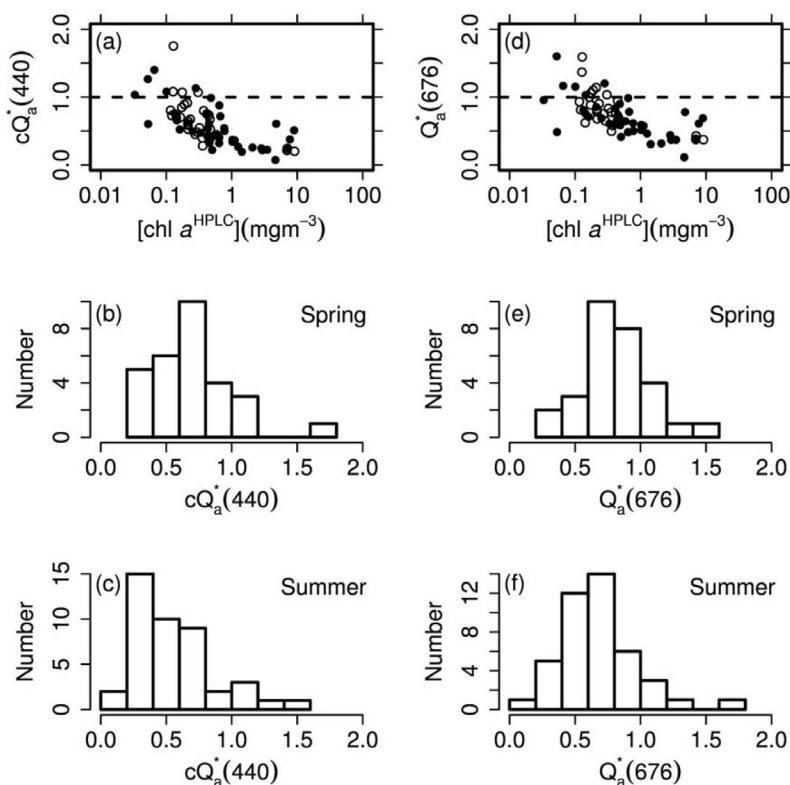


Figure 5. (a) Relationship between $[\text{chl } a^{\text{HPLC}}]$ and $cQ_a^*(440)$. Histograms of $cQ_a^*(440)$ for (b) spring and (c) summer. (d) Relationship between $[\text{chl } a^{\text{HPLC}}]$ and $Q_a^*(676)$. Histograms of $Q_a^*(676)$ for (e) spring and (f) summer. The theoretical limit (= 1) is drawn as a dashed line for Figures 5a and 5d. See Figure 3 for symbols.

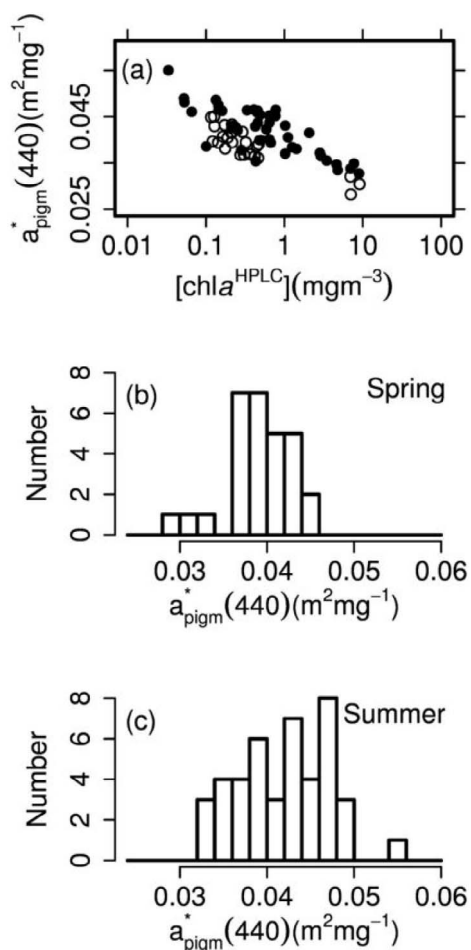


Figure 6. (a) Relationship between $a_{\text{pig}m}^*(440)$ and $[\text{chl } a^{\text{HPLC}}]$. See Figure 3 for symbols. Histogram of $a_{\text{pig}m}^*(440)$ for (b) spring and (c) summer.

photo-acclimation and/or photo-adaptation processes in Arctic waters. For the purpose of comparison with those at lower latitudes, we used the same set of figures as in Figure 3 of *Bricaud et al.* [2004]. The ratio of $[\text{chl } b]$ to $[\text{chl } a^{\text{HPLC}}]$ (denoted as $[\text{chl } b]/[\text{chl } a^{\text{HPLC}}]$) varied from 0.002 to 0.6 for both spring and summer (Figure 7a), which is comparable to variations observed at lower latitudes [*Bricaud et al.*, 2004]. The trend (i.e., magnitude and distribution) in spring was similar to that obtained in North Atlantic waters from winter to early spring (see Figure 3 of *Bricaud et al.* [2004]: denoted as POMME 1). While the magnitude of the ratio of $[\text{chl } c]$ to $[\text{chl } a^{\text{HPLC}}]$ (denoted as $[\text{chl } c]/[\text{chl } a^{\text{HPLC}}]$) and of [PSC] to $[\text{chl } a^{\text{HPLC}}]$ (denoted as $[\text{PSC}]/[\text{chl } a^{\text{HPLC}}]$) in spring was lower than that of POMME 1 (0.023 ± 0.015 and 0.336 ± 0.072 , respectively), the distribution of the scatter was similar to that of POMME 1 (Figures 7b and 7c). No clear difference between spring and summer was found. However, the ratio of [NPC] to $[\text{chl } a^{\text{HPLC}}]$ (denoted as $[\text{NPC}]/[\text{chl } a^{\text{HPLC}}]$) in summer was significantly higher than in spring ($p < 0.0001$, T-test; Figure 7d). This result indicates that during summer, the phytoplankton community was acclimated and/or adapted to higher irradiance compared to spring, increasing NPC concentrations relative to chl *a* concentrations. We note that even for summer, the values of $[\text{NPC}]/[\text{chl } a^{\text{HPLC}}]$ were remarkably low compared to those at lower latitudes [*Bricaud et al.*, 2004], but were similar to those obtained in the Labrador Sea ($0.02 < [\text{NPC}]/[\text{chl } a^{\text{HPLC}}] < 0.21$ [*Stuart et al.*, 2000]). This result is probably due to the fact that polar marine phytoplankton are generally acclimated and/or adapted to low incident light compared to those at lower latitudes [*Matsuoka et al.*, 2009], which results in their lower $[\text{NPC}]/[\text{chl } a^{\text{HPLC}}]$ values.

3.1.2. Parameterization

[29] To state the obvious, it is impossible to obtain independent information about phytoplankton absorption across the visible spectrum from ocean color sensors with a limited

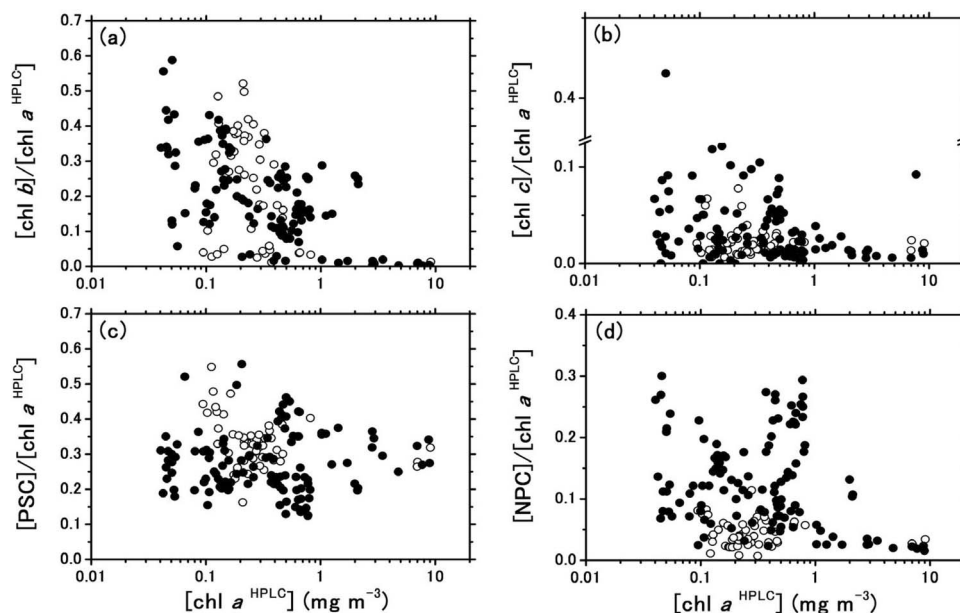


Figure 7. The ratio of (a) $[\text{chl } b]$ to $[\text{chl } a^{\text{HPLC}}]$, (b) $[\text{chl } c]$ to $[\text{chl } a^{\text{HPLC}}]$, (c) [PSC] to $[\text{chl } a^{\text{HPLC}}]$, and (d) [NPC] to $[\text{chl } a^{\text{HPLC}}]$. See Figure 3 for symbols.

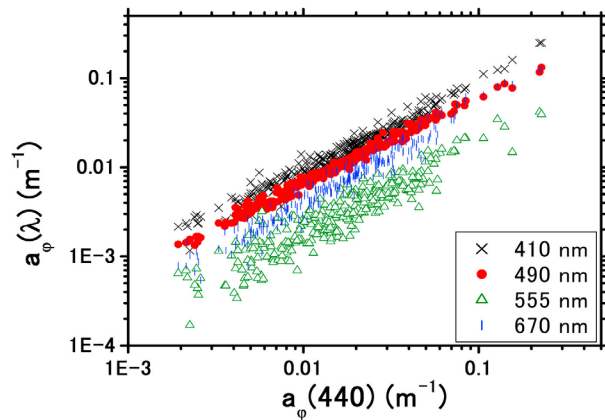


Figure 8. Relationship between $a_{\phi}(440)$ and $a_{\phi}(\lambda)$ at 410, 490, 555, and 670 nm, which approximately correspond to the wave bands of Sea-viewing Wide Field-of-view Sensor (SeaWiFS), Moderate Resolution Imaging Spectroradiometer (MODIS), and Medium-Resolution Imaging Spectrometer (MERIS) ocean color sensors. Coefficients for the regression and the coefficients of determination (r^2) are shown in Table 1.

number of wave bands. Going from estimates of absorption at one wave band (or a limited number of bands in the best case) to a spectral description of absorption therefore requires ancillary information. This information can be obtained from statistical analyses of in situ data. Here, we follow this approach and will describe the spectral absorption of phytoplankton with respect to its absorption at 440 nm, thereby assuming that it can be obtained from remote sensing [see, e.g., Matsuoka, 2008].

[30] The relationships of $a_{\phi}(440)$ versus $a_{\phi}(\lambda)$ at 410, 490, 555, and 670 nm are illustrated in Figure 8. Despite the inclusion of data from all seasons, strong coefficients of determination between each pair of bands (note that relatively lower coefficients of determination around 555 nm were found; see Table 1) were observed; no seasonal variability in these relationships was found. Our approach here is thus useful for describing $a_{\phi}(\lambda)$ over the visible spectral domain using $a_{\phi}(440)$ derived from ocean color with the statistical relationships.

3.2. CDOM and NAP Absorption

3.2.1. Seasonal Variability

[31] Values of $a_{\text{CDOM}}(440)$ varied widely in our observations ($0.0046 \text{ m}^{-1} < a_{\text{CDOM}}(440) < 0.5 \text{ m}^{-1}$; Figure 9), and fell mostly within the range observed for coastal waters around Europe [Babin et al., 2003], with the exception of the lowest values which are consistent with more open oceanic waters (e.g., 0.004 m^{-1} in the western Greenland sea [Kirk, 1994]). While differences in $a_{\text{CDOM}}(440)$ values between spring and summer were not significant, values in autumn were significantly higher than in spring and summer ($p < 0.0001$ for both; ANOVA plus TukeyHSD test). Values of the slope for CDOM absorption, S_{CDOM} , also varied widely ($0.008 \text{ nm}^{-1} < S_{\text{CDOM}}(440) < 0.033 \text{ nm}^{-1}$; Figure 9), being generally on the higher end of values published in the scientific literature [Babin et al., 2003; Twardowski et al., 2004]. The S_{CDOM}

values increased significantly between spring and summer, and then decreased strongly from summer to autumn ($p < 0.0001$ for both transition time periods, ANOVA plus TukeyHSD test).

Table 1. Coefficients for the Nonlinear Regression Expressed as $a_{\phi}(\lambda) = \alpha(\lambda)[a_{\phi}(440)]^{\beta(\lambda)}$, Where λ is the Wavelength^a

λ (nm)	$\alpha(\lambda)$	$\beta(\lambda)$	r^2
400	0.8865	1.022	0.917
405	0.9035	1.011	0.945
410	0.9318	1.008	0.961
415	0.9422	1.002	0.974
420	0.9475	0.999	0.980
425	0.9575	0.998	0.986
430	0.9614	0.992	0.989
435	0.9975	0.997	0.997
440	1.0000	1.000	1.000
445	0.8995	0.990	0.993
450	0.8550	0.989	0.993
455	0.8322	0.991	0.991
460	0.8104	0.988	0.991
465	0.8011	0.991	0.990
470	0.7434	0.979	0.989
475	0.6955	0.979	0.987
480	0.6477	0.972	0.986
485	0.6285	0.978	0.986
490	0.6031	0.981	0.985
495	0.5746	0.992	0.984
500	0.5435	0.997	0.979
505	0.5004	1.002	0.975
510	0.4622	0.999	0.967
515	0.4201	0.999	0.956
520	0.3890	0.999	0.945
525	0.3473	0.993	0.929
530	0.3315	0.999	0.918
535	0.3171	1.015	0.910
540	0.3156	1.036	0.887
545	0.2685	1.021	0.883
550	0.2422	1.023	0.850
555	0.2071	1.008	0.833
560	0.1997	1.028	0.816
565	0.1700	1.003	0.792
570	0.1685	1.013	0.791
575	0.1817	1.036	0.814
580	0.1673	1.020	0.815
585	0.1710	1.022	0.807
590	0.1709	1.025	0.826
595	0.1548	1.008	0.823
600	0.1422	0.985	0.820
605	0.1554	1.020	0.826
610	0.1738	1.039	0.859
615	0.1809	1.034	0.865
620	0.1928	1.041	0.872
625	0.2105	1.061	0.882
630	0.2043	1.042	0.885
635	0.2125	1.041	0.882
640	0.2172	1.033	0.916
645	0.2082	1.027	0.899
650	0.2416	1.064	0.913
655	0.3009	1.093	0.916
660	0.3899	1.106	0.927
665	0.5559	1.119	0.919
670	0.5930	1.094	0.929
675	0.5832	1.082	0.920
680	0.4898	1.070	0.914
685	0.2769	1.037	0.870
690	0.1450	0.983	0.845
695	0.0768	0.962	0.738
700	0.0316	0.851	0.551

^aThe coefficients of determination (r^2) are also shown.

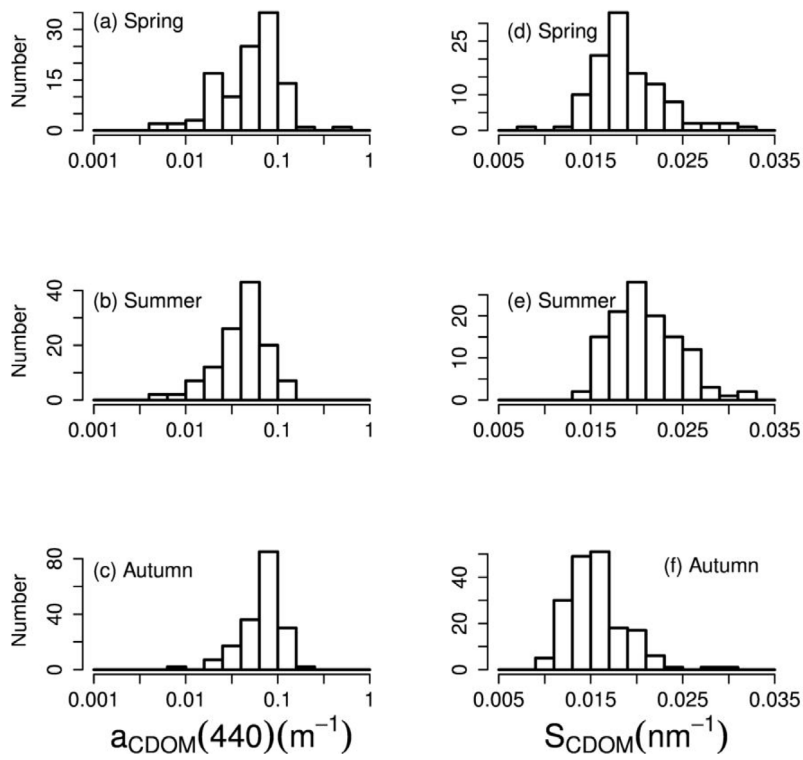


Figure 9. Histograms of $a_{CDOM}(440)$ for (a) spring, (b) summer, and (c) autumn. Histograms of S_{CDOM} for (d) spring, (e) summer, and (f) autumn.

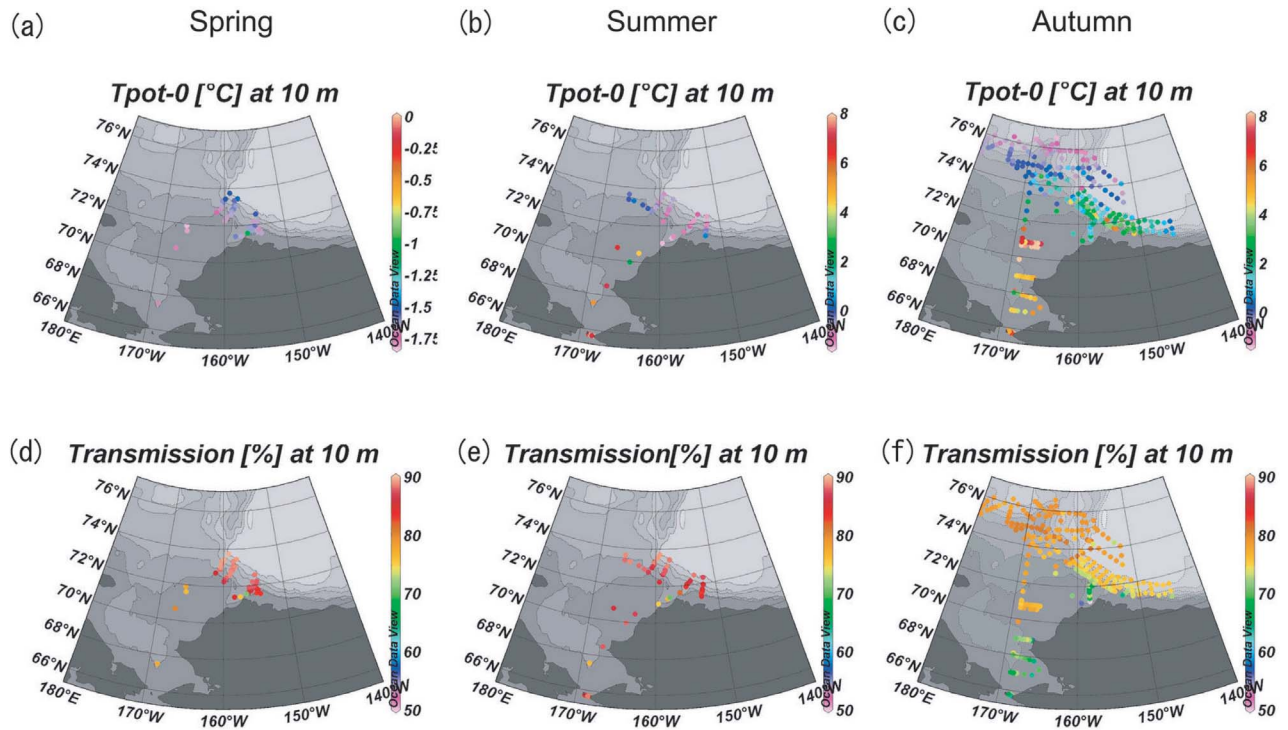


Figure 10. Potential temperature for (a) spring, (b) summer, and (c) autumn at 10 m depth. Transmission for (d) spring, (e) summer, and (f) autumn at 10 m depth.

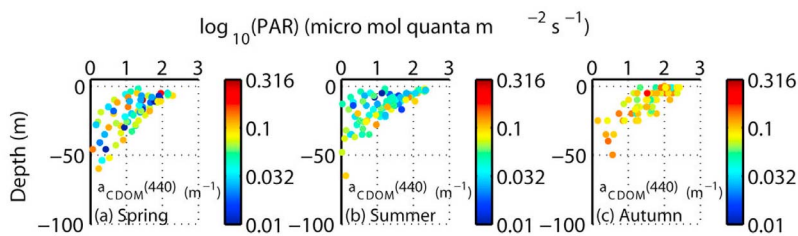


Figure 11. Vertical profile of photosynthetically available radiation (PAR) with points colored according to $a_{\text{CDOM}(440)}$ values for (a) spring, (b) summer, and (c) autumn.

[32] Alaskan Coastal Water (ACW) is an important hydrographic feature to consider in our study area in order to understand the observed variations in $a_{\text{CDOM}(440)}$. This water mass delivers large amounts of fresh water into the western Arctic, originating from the Yukon River [i.e., *Holmes et al.*, 2002; *Spencer et al.*, 2008]. Potential temperatures at 10 m depth (representative of surface water) are used as a proxy of the ACW [*Shimada et al.*, 2001; *Matsuoka et al.*, 2007] from spring to autumn, and are shown in Figure 10. In spring, the temperature on the Chukchi Sea shelf and the shelf break was generally very low and close to the freezing point ($< -1.5^{\circ}\text{C}$) (Figure 10a). The temperature in summer and autumn increased compared to spring (up to 8°C ; Figures 10b and 10c) suggesting the influence of the ACW. If the ACW was influencing CDOM absorption, the magnitude of this absorption should vary with the fractional contribution of the ACW. The ACW inflow observed in the Bering Strait is strongest in summer and declines toward

autumn [*Woodgate et al.*, 2005; *Mizobata et al.*, 2010]. However, it takes one to three months for the ACW to reach Barrow Canyon from the Bering Strait [*Weingartner et al.*, 1998]. Correspondingly, the mean value of $a_{\text{CDOM}(440)}$ in autumn was significantly higher than in summer ($p < 0.0001$, ANOVA plus TukeyHSD test; Figure 9). One possible scenario is thus that the increase in $a_{\text{CDOM}(440)}$ values from summer to autumn can be explained by the contribution of the ACW with a time lag of one to three months [*Weingartner et al.*, 1998].

[33] Figure 11 illustrates profiles of PAR as a function of depth with the points colored according to $a_{\text{CDOM}(440)}$ values. In surface waters (< 20 m at which the pycnocline was located on average), values of $a_{\text{CDOM}(440)}$ in summer were on average 34% lower than those observed in spring (Figures 11a and 11b). This result suggests that photo-bleaching occurred near the surface between spring and summer. In parallel, significant increases in S_{CDOM} values

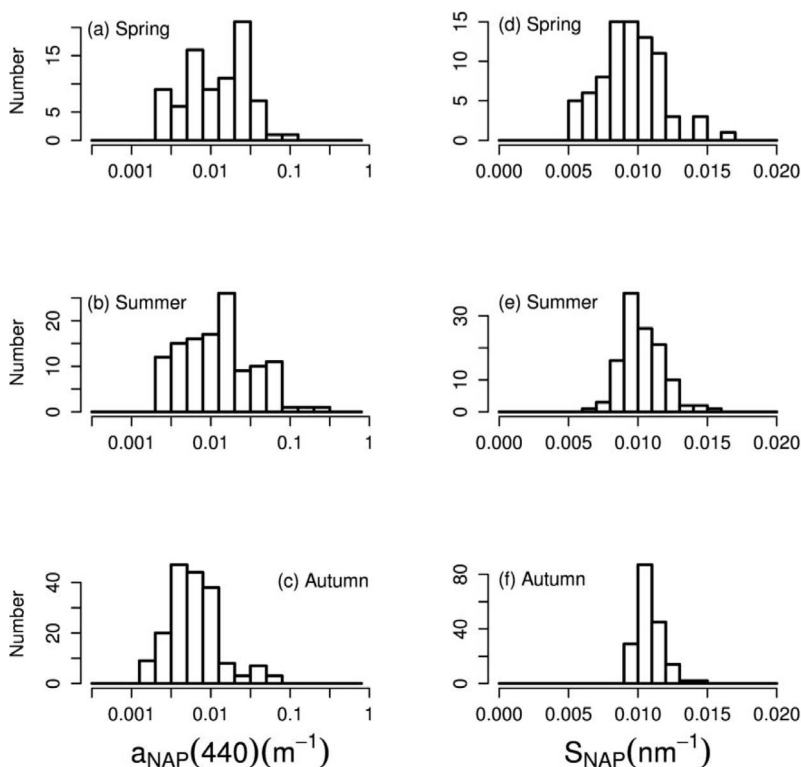


Figure 12. Histograms of $a_{\text{NAP}(440)}$ for (a) spring, (b) summer, and (c) autumn. Histograms of S_{NAP} for (d) spring, (e) summer, and (f) autumn.

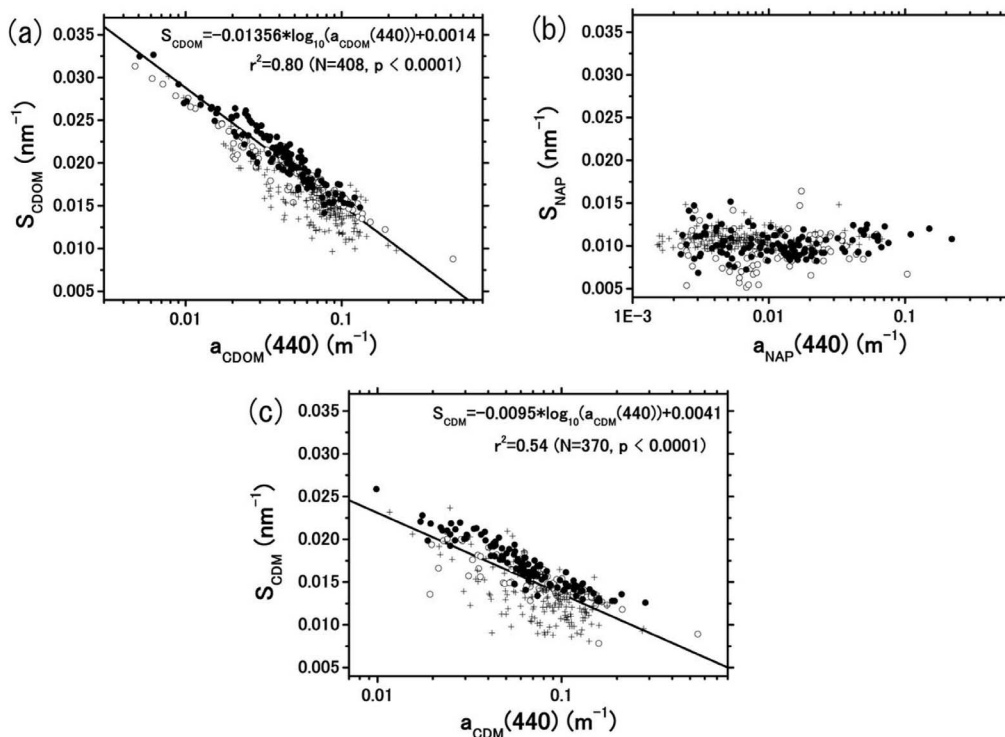


Figure 13. Relationship between the absorption coefficient and its spectral slope for (a) CDOM, (b) NAP, and (c) CDM (=CDOM + NAP) absorption. The equations for the fit for CDOM and CDM are shown. See Figure 3 for symbols.

($p < 0.0001$, T-test) were observed over the same time period. The increase in S_{CDOM} during summer is likely linked to changes in the molecular composition of CDOM caused by photobleaching, producing smaller molecules that absorb light in the shorter spectral domain [Blough and Del Vecchio, 2002; Twardowski and Donaghay, 2002]. From summer to autumn, $a_{\text{CDOM}}(440)$ values increased significantly throughout the water column ($p < 0.0001$, ANOVA plus TukeyHSD test; Figures 9e and 9f). The magnitude of $a_{\text{CDOM}}(440)$ values were higher in autumn compared to summer at all measured depths (Figures 11b and 11c), suggesting that it did not originate from locally induced vertical (i.e., wind) mixing. It is therefore likely that the increase of CDOM absorption from summer to autumn is explained by the injection of the ACW into the Arctic Ocean.

[34] Another possibility is that the magnitude of CDOM absorption was influenced by bacterial activity. In the

Arctic, bacteria can produce 11% of CDOM by consuming dissolved organic carbon [Bussmann, 1999; Kirchman *et al.*, 2005, 2007], which is consistent with laboratory experiments [e.g., Carlson and Ducklow, 1996]. If we assume that bacterial production would be greatest in the warmer summertime waters, then $a_{\text{CDOM}}(440)$ would be expected to be highest at this time. This is not the case, which may be an indication of rapid photobleaching of this material, or it could signify that bacterial production of CDOM through this pathway is not the dominant source of the observed CDOM during summer. Alternatively, the production of CDOM through phytoplankton degradation may be an important pathway during autumn as observed by the significant relationship between the chl *a* concentration and $a_{\text{CDOM}}(440)$ above one optical depth ($r^2 = 0.35$, $N = 94$; $p < 0.0001$).

Table 2. Statistics of $a_{\text{CDOM}}(\lambda)$ and $a_{\text{NAP}}(\lambda)$ at 440 nm With Their Spectral Slope, S_{CDOM} and S_{NAP} , Respectively^a

Cruise	Season	Area	$a_{\text{CDOM}}(440)$ Geometric Mean (SD)	S_{CDOM} Arithmetic Mean \pm 1 SD	$a_{\text{NAP}}(440)$ Geometric Mean (SD)	S_{NAP} Arithmetic Mean \pm 1 SD	N	
This study	SBI spring	spring	western Arctic Ocean	0.0488 (2.1754)	0.0190 ± 0.0038	0.0114 (2.4316)	0.0095 ± 0.0022	110 (80)
	SBI summer	summer	western Arctic Ocean	0.0409 (1.8720)	0.0209 ± 0.0037	0.0124 (2.7668)	0.0103 ± 0.0015	119
	MR autumn	autumn	western Arctic Ocean	0.0662 (1.6732)	0.0155 ± 0.0031	0.0062 (2.1135)	0.0108 ± 0.0009	179
	all			0.0530 (1.9337)	0.0180 ± 0.0042	0.0088 (2.5300)	0.0104 ± 0.0015	408 (378)
Babin <i>et al.</i> [2003]	COASTLOOC	–	coastal waters around Europe	0.004–0.7	0.0176 ± 0.0020	0.001–1.0	0.0123 ± 0.0013	345

^aThe geometric mean and its standard deviation (SD) are provided for $a_{\text{CDOM}}(440)$ and $a_{\text{NAP}}(440)$. The arithmetic mean and its standard deviation are provided for S_{CDOM} and S_{NAP} . The values of Babin *et al.* [2003] are also included for comparison. Note that the number of data for CDOM absorption is shown in column “N.” Also note that the number of data for NAP absorption is shown in column “N” in parentheses.

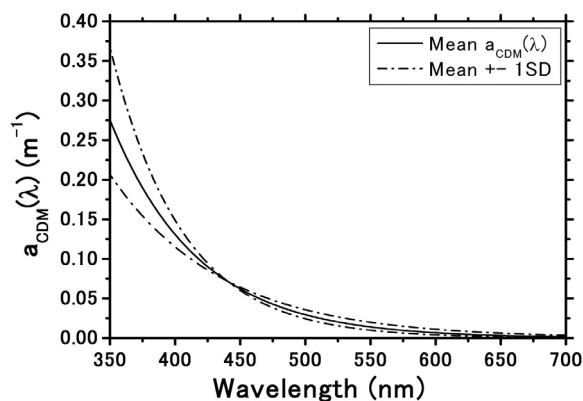


Figure 14. Computed spectra of CDM absorption. The mean values with one standard deviation are depicted as a dot-dashed curve.

[35] Values of $a_{\text{NAP}}(440)$ varied widely ($0.0016 \text{ m}^{-1} < a_{\text{NAP}}(440) < 0.22 \text{ m}^{-1}$; Figures 12a–12c), falling within the range obtained in coastal waters around Europe [Babin *et al.*, 2003]. While there was no difference in $a_{\text{NAP}}(440)$ between spring and summer, values decreased significantly from summer to autumn ($p < 0.0001$, ANOVA plus TukeyHSD test). Values of the slope for NAP absorption (S_{NAP}) also varied widely ($0.005 \text{ nm}^{-1} < S_{\text{NAP}}(440) < 0.017 \text{ nm}^{-1}$; Figures 12d–12f), and were in the lower range of values published in the literature [Nelson and Guarda, 1995; Babin *et al.*, 2003]. The S_{NAP} values increased continuously from spring to autumn ($p < 0.01$ for both spring to summer and summer to autumn, ANOVA plus TukeyHSD test).

[36] The amount of nonalgal particles is reflected by the magnitude in NAP absorption. The NAP originates from phytoplanktonic detritus, nonalgal suspended matter, or a combination of both. As seen, the chl *a* concentrations tended to decrease significantly from summer to autumn (Figure 2). If we assume that NAP originates from phytoplankton, lower NAP absorption in autumn results from the lower concentrations in the degradation products compared to summer. This hypothesis is partly supported by a significant relationship between $a_{\text{NAP}}(440)$ and the chl *a* concentration in both summer and autumn above one optical depth ($r^2 = 0.56$ and 0.54 , respectively; $p < 0.0001$ for both). Although understanding of this slope is very limited [Nelson and Guarda, 1995; Babin *et al.*, 2003; Babin and Stramski, 2004; Stramski *et al.*, 2007], a detailed study of S_{NAP} might be useful for understanding the characteristics of NAP absorption.

3.2.2. Parameterization

[37] On the basis of our analyses of CDOM absorption, we found a strong and significant inverse relationship between S_{CDOM} and $a_{\text{CDOM}}(440)$ ($r^2 = 0.80$, $p < 0.0001$, $N = 408$; Figure 13a). Although such an inverse relationship is not observed everywhere [see Babin *et al.*, 2003, Figure 5], a clear trend was reported across seasons along a transect from Delaware Bay to the Middle Atlantic Bight [e.g., Vodacek *et al.*, 1997]. This relationship was not observed for NAP absorption, with no clear relationship between S_{NAP} and $a_{\text{NAP}}(440)$ (Figure 13b). We also note that the magnitude of S_{NAP} is much smaller compared to that of S_{CDOM} (Table 2). When CDOM and NAP absorption are combined (i.e., $a_{\text{CDM}}(\lambda) = a_{\text{CDOM}}(\lambda) + a_{\text{NAP}}(\lambda)$), the slope of $a_{\text{CDM}}(440)$ (S_{CDM}) also shows an inverse relationship with $a_{\text{CDM}}(440)$ ($r^2 = 0.54$, $p < 0.0001$, $N = 370$; Figure 13c). In terms of ocean color applications, this relationship might be more useful than that for CDOM or NAP absorption alone, because decomposition of the total nonwater absorption is currently still quite difficult [e.g., International Ocean-Colour Coordinating Group, 2000]. Therefore, for a given value of $a_{\text{CDM}}(440)$, equation (5) and the relationship shown in Figure 13c, $a_{\text{CDM}}(\lambda)$ can be computed. Such a computation is presented in Figure 14 with the mean value of $a_{\text{CDM}}(440)$ and its spectral slope ± 1 SD.

[38] The high contribution of $a_{\text{CDOM}}(\lambda)$ to $a_{\text{t-w}}(\lambda)$ compared to $a_{\text{NAP}}(\lambda)$ is clearly shown (Table 3). In particular, the proportion of $a_{\text{CDOM}}(\lambda)$ to $a_{\text{t-w}}(\lambda)$ at 440 nm was high across seasons (from spring to autumn), contributing on average 66% of the total nonwater absorption (Table 3). This result is consistent with previous findings [e.g., Siegel *et al.*, 2002; Nelson and Siegel, 2002; Bélanger *et al.*, 2006; Matsuoka *et al.*, 2007, 2009; Brown *et al.*, 2008], where a high contribution of CDOM absorption at higher latitudes was observed. It should be noted that even though the contribution of phytoplankton absorption to the total nonwater absorption is smaller than that of CDOM absorption, variability in the phytoplankton absorption is larger than that of CDOM. This is the main cause of the failure of global ocean color algorithms when applied to the Arctic Ocean [Matsuoka *et al.*, 2007]. Because the relative contribution of $a_{\text{CDOM}}(\lambda)$ to $a_{\text{t-w}}(\lambda)$ is high but relatively constant, ocean color algorithms can be corrected for high $a_{\text{CDOM}}(\lambda)$ values by developing regionally specific relationships between the chl *a* concentration and a reflectance ratio (or water-leaving radiance ratio).

4. Conclusions

[39] In the present study, we examined and parameterized the absorption properties of optically significant components

Table 3. Relative Contribution of the Absorption Coefficient of Phytoplankton ϕ , NAP, and CDOM to the Total Nonwater Absorption at 440 nm^a

	Cruise	Season	$a_{\phi}(440)/a_{\text{t-w}}(440)$	$a_{\text{CDOM}}(440)/a_{\text{t-w}}(440)$	$a_{\text{NAP}}(440)/a_{\text{t-w}}(440)$	N
This study	SBI spring	spring	0.22 ± 0.12	0.63 ± 0.17	0.14 ± 0.10	61
	SBI summer	summer	0.29 ± 0.13	0.55 ± 0.15	0.16 ± 0.09	109
	MR autumn	autumn	0.18 ± 0.12	0.73 ± 0.14	0.09 ± 0.05	179
	all		0.22 ± 0.13	0.66 ± 0.17	0.12 ± 0.08	349
Babin <i>et al.</i> [2003]	COASTLOOC		0.36 ± 0.14	0.41 ± 0.14	0.22 ± 0.13	345

^aThe values of Babin *et al.* [2003] are also included for comparison.

in western Arctic waters using in situ data sets from spring to autumn. We found that the relationship between the chl *a* concentration and phytoplankton absorption at 440 nm across seasons is similar to that observed at lower latitudes. However, seasonal variability in chl *a*-specific phytoplankton absorption was identified. The lower chl *a*-specific absorption coefficient of phytoplankton from spring to summer is attributed to a strong package effect overwhelming the influence of the pigment composition. This effect is the main cause of the failure of the retrieval of the chl *a* concentration using global ocean color algorithms at high northern latitudes [Matsuoka *et al.*, 2007]. Retrieval of the chl *a* concentration is the basis for many biogeochemical products (e.g., primary production, carbon flux), which are vital for furthering our understanding of the impacts and feedbacks of climate change on the ecology of not just the western Arctic Ocean, but also on a Pan-Arctic scale.

[40] Similar to the phytoplankton absorption, CDOM and NAP absorption also showed significant seasonal variations. A decrease in $a_{\text{CDOM}}(440)$ values near the surface from spring to summer, and an associated increase in S_{CDOM} values, is explained by photobleaching. An increase in the magnitude of a_{CDOM} from summer to autumn is postulated to be a combination of the cumulative injection of the ACW inflow in addition to the in situ production of CDOM originating from the degradation of phytoplankton. The decrease in NAP absorption toward autumn could reflect the decrease in the concentration of phytoplanktonic detritus which results from a lower phytoplankton biomass.

[41] In terms of ocean color applications, $a_{\phi}(440)$ can be simply estimated using either empirical or semi-analytical relationships with remote sensing reflectance or normalized water-leaving radiance [e.g., Stramska *et al.*, 2003; Lee *et al.*, 2002; Matsuoka, 2008]. Consistency in the relationship between $a_{\phi}(440)$ and $a_{\phi}(\lambda)$ means that it is also possible to obtain spectral measurements of $a_{\phi}(\lambda)$ using space-based ocean color sensors. Detailed spectra of $a_{\phi}(\lambda)$ can be useful for spectral primary production models. In terms of bottom-up control, this knowledge can open the door to understanding temporal and spatial changes in the Arctic ecosystem as consequences of ongoing global warming using satellite remote sensing.

Appendix A: Comparison of the Slope for CDOM Absorption Obtained Using a Linear Model and a Nonlinear Model

[42] In the literature, the spectral slope for CDOM absorption was often calculated by fitting a linear model to the log-transformed $a_{\text{CDOM}}(\lambda)$ from 350 to 500 nm [e.g., Matsuoka *et al.*, 2007]. However, several studies have stated that nonlinear fitting is better [e.g., Babin *et al.*, 2003; Twardowski *et al.*, 2004]. To examine the bias, we compared the spectral slopes using linear and nonlinear fitting techniques for both oceanic and coastal waters. For nonlinear fitting, we used an exponential model (equation (5)) within the spectral domain from 350 to 500 nm [Babin *et al.*, 2003]. Our results, in agreement with those of Twardowski *et al.* [2004], show that S_{CDOM} values using the nonlinear model tend to be higher than those using the linear one (Figure A1). This results from the fact that a linear fit on log-transformed $a_{\text{CDOM}}(\lambda)$ values gives more statistical weight to relatively low values in the

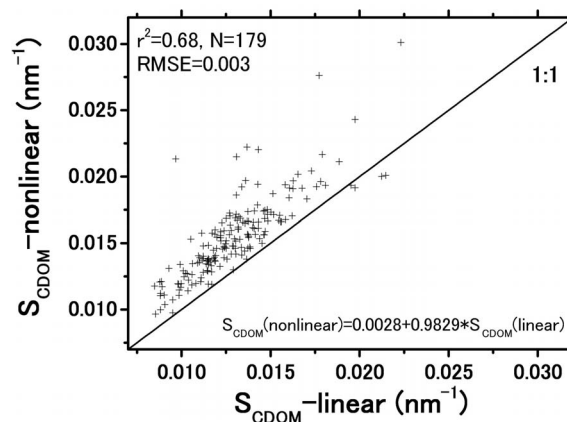


Figure A1. Relationship between S_{CDOM} calculated using a linear fitting method and a nonlinear fitting method.

visible spectral domain than does the nonlinear regression [Babin *et al.*, 2003]. As a conclusion, we suggest that a nonlinear fit to calculate a spectral slope for CDOM should be used systematically for all available data to exclude a potential bias.

[43] **Acknowledgments.** This research was supported by the Japan Aerospace Exploration Agency (JAXA) through the program of Arctic research projects using International Arctic Research Center–JAXA Information System (IARC-IJIS), the Arctic System Sciences program of the National Science Foundation OPP-0125049 and 0223375, and NASA’s Sensor Intercomparison and Merger for Biological and Interdisciplinary Studies (SIMBIOS) program NAG5-10528. We are grateful to the captain and crews of the *USCGC Healy* and Japanese R/V *Mirai* for their assistance in the collection of data for this study. CTD data during the SBI spr and SBI sum cruises were obtained from <http://www.eol.ucar.edu/projects/sbi/on> the basis of the data policy. Comments by three anonymous reviewers and C. Brown have greatly helped in improving the manuscript.

References

- Antoine, D., and A. Morel (1996), Oceanic primary production: 1. Adaptation of a spectral light-photosynthesis model in view of application to satellite chlorophyll observations, *Global Biogeochem. Cycles*, *10*, 43–55.
- Arrigo, K. R., D. Worthen, A. Schnell, and M. P. Lizotte (1998), Primary production in Southern Ocean waters, *J. Geophys. Res.*, *103*, 15,587–15,600, doi:10.1029/98JC00930.
- Babin, M., and D. Stramski (2004), Variations in the mass-specific absorption coefficient of mineral particles suspended in water, *Limnol. Oceanogr.*, *49*(3), 756–767, doi:10.4319/lo.2004.49.3.0756.
- Babin, M., A. Morel, and B. Gentili (1996), Remote sensing of sea surface Sun-induced chlorophyll fluorescence: Consequences of natural variations in the optical characteristics of phytoplankton and the quantum yield of chlorophyll *a* fluorescence, *Int. J. Remote Sens.*, *17*, 2417–2448, doi:10.1080/01431169608948781.
- Babin, M., D. Stramski, G. M. Ferrari, H. Claustre, A. Bricaud, G. Obolensky, and N. Hoepffner (2003), Variations in the light absorption coefficients of phytoplankton, nonalgal particles, and dissolved organic matter in coastal waters around Europe, *J. Geophys. Res.*, *108*(C7), 3211, doi:10.1029/2001JC000882.
- Behrenfeld, M. J., and P. G. Falkowski (1997), Photosynthetic rates derived from satellite-based chlorophyll concentration, *Limnol. Oceanogr.*, *42*(1), 1–20, doi:10.4319/lo.1997.42.1.0001.
- Behrenfeld, M. J., E. Boss, D. A. Siegel, and D. M. Shea (2005), Carbon-based ocean productivity and phytoplankton physiology from space, *Global Biogeochem. Cycles*, *19*, GB1006, doi:10.1029/2004GB002299.
- Bélangier, S., H. Xie, N. Krotkov, P. Larouche, W. F. Vincent, and M. Babin (2006), Photomineralization of terrigenous dissolved organic matter in Arctic coastal waters from 1979 to 2003: Interannual variability and implications of climate change, *Global Biogeochem. Cycles*, *20*, GB4005, doi:10.1029/2006GB002708.
- Bidigare, R. R., and C. C. Trees (2000), HPLC phytoplankton pigments: Sampling laboratory methods, and quality assurance procedures, in

- Ocean Optics Protocols for Satellite Ocean Color Sensor Validation, Revision 2, NASA Tech. Rep., 2000–209966*, edited by G. S. Fargion and J. L. Mueller, pp. 154–161, Goddard Space Flight Cent., Greenbelt, Md.
- Bidigare, R. R., M. E. Ondrusek, J. H. Morrow, and D. A. Kiefer (1990), In vivo absorption properties of algal pigments, *Proc. SPIE*, 1302, 290–302, doi:10.1117/12.21451.
- Blough, N. V., and R. Del Vecchio (2002), Chromophoric DOM in the open ocean, in *Biogeochemistry of Marine Dissolved Organic Matter*, edited by D. A. Hansell and C. A. Carlson, pp. 509–546, doi:10.1016/B978-012323841-2/50012-9, Academic, Boston.
- Bricaud, A., and A. Morel (1983), Optical efficiency factors of some phytoplankters, *Limnol. Oceanogr.*, 28(5), 816–832, doi:10.4319/lo.1983.28.5.0816.
- Bricaud, A., A. Morel, and L. Prieur (1981), Absorption by dissolved organic matter of the sea (yellow substance) in the UV and visible domains, *Limnol. Oceanogr.*, 26(1), 43–53, doi:10.4319/lo.1981.26.1.0043.
- Bricaud, A., M. Babin, A. Morel, and H. Claustre (1995), Variability in the chlorophyll-specific absorption coefficients of natural phytoplankton: Analysis and parameterization, *J. Geophys. Res.*, 100, 13,321–13,332, doi:10.1029/95JC00463.
- Bricaud, A., A. Morel, M. Babin, K. Allai, and H. Claustre (1998), Variations of light absorption by suspended particles with chlorophyll a concentration in oceanic (case 1) waters: Analysis and implications for bio-optical models, *J. Geophys. Res.*, 103, 31,033–31,044, doi:10.1029/98JC02712.
- Bricaud, A., H. Claustre, J. Ras, and K. Oubelkheir (2004), Natural variability of phytoplanktonic absorption in oceanic waters: Influence of the size structure of algal populations, *J. Geophys. Res.*, 109, C11010, doi:10.1029/2004JC002419.
- Brown, C., Y. Huot, P. J. Wendell, B. Gentili, and H. Claustre (2008), The origin and global distribution of second order variability in satellite ocean color and its potential applications to algorithm development, *Remote Sens. Environ.*, 112, 4186–4203, doi:10.1016/j.rse.2008.06.008.
- Bussmann, H. (1999), Bacterial utilization of humic substances from the Arctic Ocean, *Aquat. Microb. Ecol.*, 19, 37–45, doi:10.3354/ame019037.
- Campbell, J. W. (1995), The lognormal distribution as a model for bio-optical variability in the sea, *J. Geophys. Res.*, 100, 13,237–13,254, doi:10.1029/95JC00458.
- Carlson, C. A., and H. W. Ducklow (1996), Growth of bacterioplankton and consumption of dissolved organic carbon in the Sargasso Sea, *Aquat. Microb. Ecol.*, 10, 69–85, doi:10.3354/ame010069.
- Carmack, E., R. W. Macdonald, and S. Jasper (2004), Phytoplankton productivity on the Canadian Shelf of the Beaufort Sea, *Mar. Ecol. Prog. Ser.*, 277, 37–50, doi:10.3354/meps277037.
- Chen, M., H. Yipu, G. Laodong, C. Pingphe, Y. Weifeng, L. Guangshan, and Q. Yusheng (2002), Biological productivity and carbon cycling in the Arctic Ocean, *Chin. Sci. Bull.*, 47, 1037–1040.
- Cleveland, J. S., and A. D. Weidemann (1993), Quantifying absorption by aquatic particles: A multiple scattering correction for glass-fiber filters, *Limnol. Oceanogr.*, 38(6), 1321–1327, doi:10.4319/lo.1993.38.6.1321.
- Cota, G. F., W. G. Harrison, T. Platt, S. Sathyendranath, and V. Stuart (2003), Bio-optical properties of the Labrador Sea, *J. Geophys. Res.*, 108(C7), 3228, doi:10.1029/2000JC000597.
- Cota, G. F., J. Wang, and J. C. Comiso (2004), Transformation of global satellite chlorophyll retrievals with a regionally tuned algorithm, *Remote Sens. Environ.*, 90, 373–377, doi:10.1016/j.rse.2004.01.005.
- Hill, V. (2008), Impacts of chromophoric dissolved organic material on surface ocean heating in the Chukchi Sea, *J. Geophys. Res.*, 113, C07024, doi:10.1029/2007JC004119.
- Hill, V., and G. Cota (2005), Spatial patterns of primary production on the shelf, slope and basin of the Western Arctic in 2002, *Deep Sea Res. Part II*, 52, 3344–3354, doi:10.1016/j.dsr2.2005.10.001.
- Hill, V., G. Cota, and D. Stockwell (2005), Spring and summer phytoplankton communities in the Chukchi and Eastern Beaufort seas, *Deep Sea Res. Part II*, 52, 3369–3385, doi:10.1016/j.dsr2.2005.10.010.
- Holmes, R. M., J. W. McClelland, B. J. Peterson, I. A. Shiklomanov, A. I. Shiklomanov, A. V. Zhulidov, V. V. Gordeev, and N. N. Bobrovitskaya (2002), A circum-polar perspective on fluvial sediment flux to the Arctic Ocean, *Global Biogeochem. Cycles*, 16(4), 1098, doi:10.1029/2001GB001849.
- Holm-Hansen, O., C. J. Lorenzen, R. W. Holms, and J. D. H. Strickland (1965), Fluorometric determination of chlorophyll, *J. Cons. Int. Explor. Mer.*, 30, 3–15.
- International Ocean-Colour Coordinating Group (2000), Remote sensing of ocean colour in coastal, and optically complex, waters, in *Reports of the International Ocean-Colour Coordinating Group*, vol. 3, edited by S. Sathyendranath, pp. 1–22, Dartmouth, N. S., Canada.
- Johnsen, G., O. Samset, L. Granskog, and E. Sakshaug (1994), In vivo absorption characteristics in 10 classes of bloom-forming phytoplankton: Taxonomic characteristics and response to photoadaptation by means of discriminant and HPLC analysis, *Mar. Ecol. Prog. Ser.*, 105, 149–157, doi:10.3354/meps105149.
- Kirchman, D. L., R. R. Malmstrom, and M. T. Cottrell (2005), Control of bacterial growth by temperature and organic matter in the Western Arctic, *Deep Sea Res. Part II*, 52, 3386–3395, doi:10.1016/j.dsr2.2005.09.005.
- Kirchman, D. L., H. Elifantz, A. I. Dittel, R. R. Malmstrom, and M. T. Cottrell (2007), Standing stocks and activity of archaea and bacteria in the western Arctic Ocean, *Limnol. Oceanogr.*, 52(2), 495–507, doi:10.4319/lo.2007.52.2.0495.
- Kirk, J. T. O. (1994), *Light and Photosynthesis in Aquatic Ecosystems*, 2nd ed., doi:10.1017/CBO9780511623370, Cambridge Univ. Press, New York.
- Kishino, M., M. Takahashi, N. Okami, and S. Ishimaru (1985), Estimation of the spectral absorption coefficients of phytoplankton in the sea, *Bull. Mar. Sci.*, 37, 634–642.
- Lee, Z. P., K. L. Carder, and R. A. Arnone (2002), Deriving inherent optical properties from water color: A multiband quasi-analytical algorithm for optically deep waters, *Appl. Opt.*, 41, 5755–5772, doi:10.1364/AO.41.005755.
- Longhurst, A., S. Sathyendranath, T. Platt, and C. Caverhill (1995), An estimate of global primary production in the ocean from satellite radiometer data, *J. Plankton Res.*, 17, 1245–1271, doi:10.1093/plankt/17.6.1245.
- Lovejoy, C., W. Vincent, S. Bonilla, S. Roy, M.-J. Martineau, R. Terrado, M. Potvin, R. Messana, and C. Pedos-Alio (2007), Distribution, phylogeny, and growth of cold-adapted picoplankton in Arctic seas, *J. Phycol.*, 43, 78–89, doi:10.1111/j.1529-8817.2006.00310.x.
- Matsuoka, A. (2008), Bio-optical characteristics of the Arctic Ocean: Application to an Arctic Ocean color algorithm, Ph.D. thesis, Hokkaido Univ., Sapporo, Japan.
- Matsuoka, A., Y. Huot, K. Shimada, S. Saitoh, and M. Babin (2007), Bio-optical characteristics of the western Arctic Ocean: Implications for ocean color algorithms, *Can. J. Remote Sens.*, 33, 503–518.
- Matsuoka, A., P. Larouche, M. Poulin, W. Vincent, and H. Hattori (2009), Phytoplankton community adaptation to changing light levels in the southern Beaufort Sea, Canadian Arctic, *Estuarine Coastal Shelf Sci.*, 82, 537–546, doi:10.1016/j.ecss.2009.02.024.
- Mitchell, B. G. (1992), Predictive bio-optical relationships for polar oceans and marginal ice zones, *J. Mar. Syst.*, 3, 91–105, doi:10.1016/0924-7963(92)90032-4.
- Mitchell, B. G., M. Kahru, J. Wieland, and M. Stramska (2003), Determination of spectral absorption coefficients of particles, dissolved materials and phytoplankton for discrete water samples, in *Ocean Optics Protocols for Satellite Ocean Color Sensor Validation, Revision 4*, vol. 4, *Inherent Optical Properties: Instruments, Characterization, Field Measurements and Data Analysis Protocols, NASA Tech. Rep. 2003-211621*, edited by J. L. Mueller, G. S. Fargion, and C. R. McClain, pp. 39–64, Goddard Space Flight Cent., Greenbelt, Md.
- Mizobata, K., K. Shimada, R. Woodgate, S. Saitoh, and J. Wang (2010), Estimation of heat flux through the eastern Bering Strait, *J. Oceanogr.*, 66, 405–424, doi:10.1007/s10872-010-0035-7.
- Morel, A. (1978), Available, usable, and stored radiant energy in relation to marine photosynthesis, *Deep Sea Res.*, 25, 673–688, doi:10.1016/0146-6291(78)90623-9.
- Morel, A. (1988), Optical modeling of the upper ocean in relation to its biogenous matter content (case 1 waters), *J. Geophys. Res.*, 93, 10,749–10,768, doi:10.1029/JC093iC09p10749.
- Morel, A. (1991), Light and marine photosynthesis: A spectral model with geochemical and climatological implications, *Prog. Oceanogr.*, 26, 263–306, doi:10.1016/0079-6611(91)90004-6.
- Morel, A., and A. Bricaud (1981), Theoretical results concerning light absorption in a discrete medium, and application to specific absorption of phytoplankton, *Deep Sea Res. Part A*, 28, 1375–1393, doi:10.1016/0198-0149(81)90039-X.
- Nelson, J. R., and S. Guarda (1995), Particulate and dissolved spectral absorption on the continental shelf of the northern United States, *J. Geophys. Res.*, 100, 8715–8732, doi:10.1029/95JC00222.
- Nelson, N. B., and D. A. Siegel (2002), Chromophoric DOM in the open ocean, in *Biogeochemistry of Marine Dissolved Organic Matter*, edited by D. A. Hansell and C. A. Carlson, pp. 547–578, doi:10.1016/B978-012323841-2/50013-0, Academic, Boston.
- Pabi, S., G. L. van Dijken, and K. Arrigo (2008), Primary production in the Arctic Ocean, 1998–2006, *J. Geophys. Res.*, 113, C08005, doi:10.1029/2007JC004578.
- Perovich, D. K., B. Light, H. Eiken, K. F. Jones, and K. Runciman (2007), Increasing solar heating of the Arctic Ocean and adjacent seas, 1979–2005: Attribution and role in the ice-albedo-feedback, *Geophys. Res. Lett.*, 34, L19505, doi:10.1029/2007GL031480.

- Platt, T., and S. Sathyendranath (1988), Oceanic primary production: Estimation by remote sensing at local and regional scales, *Science*, *241*, 1613–1620, doi:10.1126/science.241.4873.1613.
- Retamal, L., S. Bonilla, and W. Vincent (2008), Optical gradients and phytoplankton production in the Mackenzie River and the coastal Beaufort Sea, *Polar Biol.*, *31*, 363–379, doi:10.1007/s00300-007-0365-0.
- Sakshaug, E. (2004), Primary and secondary production in the Arctic seas, in *The Organic Carbon Cycle in the Arctic Ocean*, edited by R. Stein and R. Macdonald, pp. 57–81, Springer, New York.
- Sathyendranath, S., T. Platt, E. P. W. Horne, W. G. Harrison, O. Ulloa, R. Outerbridge, and N. Hoepffner (1991), Estimation of new production in the ocean by compound remote sensing, *Nature*, *353*, 129–133, doi:10.1038/353129a0.
- Shiklomanov, I. A. (1993), World fresh water resources, in *Water in Crisis: A Guide to the World's Fresh Water Resources*, edited by P. H. Gleick, pp. 13–24, Oxford Univ. Press, New York.
- Shimada, K., E. C. Carmack, K. Hatakeyama, and T. Takizawa (2001), Varieties of shallow temperature maximum waters in the western Canadian Basin of the Arctic Ocean, *Geophys. Res. Lett.*, *28*, 3441–3444, doi:10.1029/2001GL013168.
- Shimada, K., T. Kamoshida, M. Itoh, S. Nishino, E. Carmack, F. McLaughlin, S. Zimmermann, and A. Proshutinsky (2006), Pacific Ocean inflow: Influence on catastrophic reduction of sea ice cover in the Arctic Ocean, *Geophys. Res. Lett.*, *33*, L08605, doi:10.1029/2005GL025624.
- Siegel, D. A., S. Maritorena, N. B. Nelson, D. A. Hansell, and M. Lorenzi-Kayser (2002), Global distribution and dynamics of colored dissolved and detrital organic materials, *J. Geophys. Res.*, *107*(C12), 3228, doi:10.1029/2001JC000965.
- Sokal, R. R., and F. J. Rohlf (1973), *Introduction to Biostatistics*, Dover, Mineola, N. Y.
- Spencer, R. G. M., G. R. Aiken, K. P. Wickland, R. G. Striegl, and P. J. Hernes (2008), Seasonal and spatial variability in dissolved organic matter quantity and composition from the Yukon River basin, Alaska, *Global Biogeochem. Cycles*, *22*, GB4002, doi:10.1029/2008GB003231.
- Stramska, M., D. Stramski, R. Hapter, S. Kaczmarek, and J. Ston (2003), Bio-optical relationships and ocean color algorithms for the north polar region of the Atlantic, *J. Geophys. Res.*, *108*(C5), 3143, doi:10.1029/2001JC001195.
- Stramska, M., D. Stramski, S. Kaczmarek, D. B. Allison, and J. Schwarz (2006), Seasonal and regional differentiation of bio-optical properties within the north polar Atlantic, *J. Geophys. Res.*, *111*, C08003, doi:10.1029/2005JC003293.
- Stramski, D., M. Babin, and S. B. Wozniak (2007), Variations in the optical properties of terrigenous mineral-rich particulate matter suspended in seawater, *Limnol. Oceanogr.*, *52*(6), 2418–2433, doi:10.4319/lo.2007.52.6.2418.
- Stroeve, J., M. Serreze, S. Drobot, S. Gearheard, M. Holland, J. Maslanik, W. Meier, and T. Scambos (2008), Arctic sea ice extent plummets in 2007, *Eos Trans. AGU*, *89*(2), 13–14, doi:10.1029/2008EO020001.
- Stuart, V., S. Sathyendranath, E. J. H. Head, T. Platt, B. Ivin, and H. Maass (2000), Bio-optical characteristics of diatom and prymnesiophyte populations in the Labrador Sea, *Mar. Ecol. Prog. Ser.*, *201*, 91–106, doi:10.3354/meps201091.
- Suzuki, R., and T. Ishimaru (1990), An improved method for the determination of phytoplankton chlorophyll using n,n-dimethylformamide, *J. Oceanogr.*, *46*, 190–194.
- Twardowski, M. S., and P. L. Donaghay (2002), Photo-bleaching of aquatic dissolved materials: Absorption removal, spectral alteration, and their interrelationship, *J. Geophys. Res.*, *107*(C8), 3091, doi:10.1029/1999JC000281.
- Twardowski, M. S., E. Boss, J. M. Sullivan, and P. L. Donaghay (2004), Modeling the spectral shape of absorption by chromophoric dissolved organic matter, *Mar. Chem.*, *89*, 69–88, doi:10.1016/j.marchem.2004.02.008.
- Vodacek, A., N. V. Blough, M. D. DeGranpre, E. T. Peltzer, and R. K. Nelson (1997), Seasonal variations of CDOM and DOC in the Middle Atlantic Bight: Terrestrial inputs and photooxidation, *Limnol. Oceanogr.*, *42*(4), 674–686, doi:10.4319/lo.1997.42.4.0674.
- Wang, J., G. F. Cota, and D. A. Ruble (2005), Absorption and backscattering in the Beaufort and Chukchi seas, *J. Geophys. Res.*, *110*, C04014, doi:10.1029/2002JC001653.
- Weingartner, T. J., D. J. Cavalieri, K. Aagaard, and Y. Sasaki (1998), Circulation, dense water formation, and outflow on the northeast Chukchi shelf, *J. Geophys. Res.*, *103*, 7647–7661, doi:10.1029/98JC00374.
- Woodgate, R. A., K. Aagaard, and T. J. Weingartner (2005), Monthly temperature, salinity, and transport variability of the Bering Strait through flow, *Geophys. Res. Lett.*, *32*, L04601, doi:10.1029/2004GL021880.
- Wright, S. W., S. W. Jeffrey, R. F. C. Mantoura, C. A. Llewellyn, T. Bjornland, D. Repeta, and N. Welschmeyer (1991), Improved HPLC method for the analysis of chlorophylls and carotenoids from marine phytoplankton, *Mar. Ecol. Prog. Ser.*, *77*, 183–196, doi:10.3354/meps077183.

M. Babin, Québec-Océan, Université Laval, Pavillon Alexandre-Vachon 1045, Avenue de la Médecine, Local 2078, Québec City, QC G1V 0A6, Canada.

A. Bricaud and A. Matsuoka, Laboratoire d'Océanographie de Villefranche, Université Pierre et Marie Curie, Centre National de la Recherche Scientifique, B.P. 08, Port de la Darse, Villefranche-sur-Mer, F-06230 France. (anick@obs-vlfr.fr; atsushi.matsuoka@obs-vlfr.fr)

V. Hill, Ocean, Earth, and Atmospheric Sciences, Old Dominion University, 4600 Elkhorn Ave., Norfolk, VA 23529, USA. (vhill@odu.edu)

Y. Huot, Centre d'Applications et de Recherches en Télédétection, Département de Géomatique Appliquée, Université de Sherbrooke, Sherbrooke, QC J1K 2R1, Canada. (yannick.huot@usherbrooke.ca)